INVERSE PROBLEMS IN GEOPHYSICAL APPLICATIONS

Edited by **Heinz W. Engl**
Institute für Mathematik
Johannes Kepler Universitdt
Linz, Austria

Alfred K. Louis
Universität des Saarlandes
Saarbrücken, Germany

William Rundell
Texas A & M University
College Station, Texas

siam
Society for Industrial and
Applied Mathematics
Philadelphia

The Inversion of Body-Wave Attributes Derived From Seismic Refraction Data

Robert L. Nowack*

Michael P. Matheney*

Abstract

An inversion formulation for crustal structure using seismic attributes has been developed. The seismic attributes include envelope amplitude, instantaneous frequency and phase time of selected seismic phases. Complex trace analysis is used to extract different seismic attributes from the seismic data. For the inversion of seismic attributes, ray perturbation is utilized to compute the sensitivity of different attributes to changes in the model. An iterative procedure is then performed from smooth to less-smooth models which progressively incorporates the longer wavelength components of the model. To illustrate the method, seismic refraction data from the Ouachita PASSCAL and the Glimpce Lake Superior experiments are used to invert for crustal velocity and attenuation structure.

1 Introduction

The inversion of seismic attributes for crustal structure is an alternative to the direct inversion of seismic wavefield data which can be highly nonlinear. Attribute inversion also incorporates more of the seismic data than using only travel-times. Examples of seismic attributes include envelope amplitudes and instantaneous frequencies, as well as the phase times of selected arrivals. The extraction of seismic attributes is performed using complex trace analysis, however, a more general wavelet analysis could also be used.

To invert for seismic attributes, ray perturbation methods are utilized to compute the sensitivity of different attributes to changes in the model. An iterative procedure, which progressively incorporates the longer wavelength features of the model, from smooth models to less-smooth models, is then performed. When inverting attributes, such as amplitudes and instantaneous frequencies, the subsurface model must include both velocity and attenuation structure. To illustrate the inversion of seismic attributes for laterally varying structure, attributes extracted from refraction data from the Ouachita PASSCAL and Glimpce Lake Superior experiments are used to invert for crustal velocity and attenuation structure.

*Dept. of Earth & Atmospheric Sciences, Purdue University, West Lafayette, IN 47907-1397.

2. Extraction of Seismic Attributes

The extraction of seismic attributes can be performed by complex trace analysis, as well as by more general wavelet analysis [8]. The approach followed here is to perform complex trace analysis in which the analytic signal is constructed from the seismic trace. From the analytic signal, the envelope and instantaneous frequency can be determined. Applications of complex trace analysis to seismic data have been described in [32]. The resulting instantaneous frequency is, in general, not equivalent to a spectral frequency. However, when a weighted average of the instantaneous frequency is performed, using the squared amplitude, the estimate converges to the positive spectral frequency [7].

Figure 1 shows an example of the determination of the complex envelope and instantaneous frequency from an observed seismic trace. The phase times are extracted from either the onset time or peak amplitude of the envelope of selected seismic phases. The envelope peak amplitude and instantaneous frequencies are then extracted for the selected arrival.

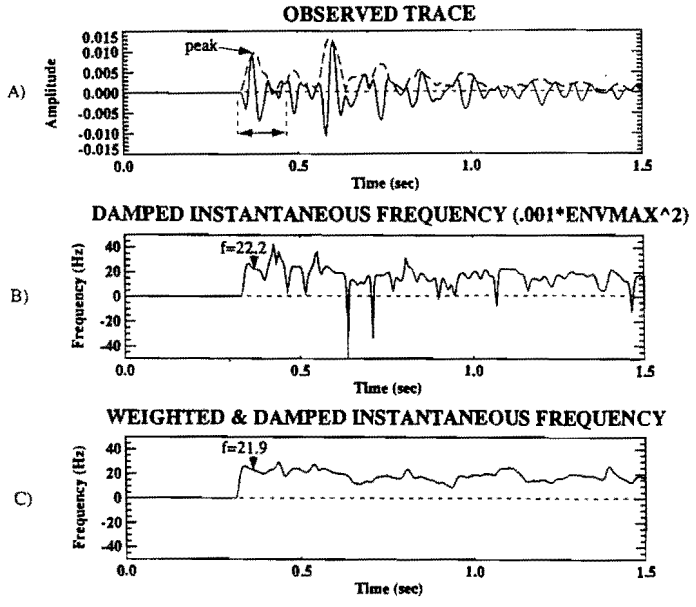

Fig. 1. *A) an observed seismic trace and its complex envelope. B) Damped instantaneous frequency of the seismic trace in A). C) Weighted and damped instantaneous frequency. For a peak of the first arrival envelope, the instantaneous frequency is noted.*

In order to obtain values of the attenuation factor t^*, a matching procedure of the instantaneous frequencies between the observed data and an attenuated reference pulse is performed [15]. In this approach, a reference pulse is attenuated to the distance of the

receiver. The instantaneous frequency is then computed for the observed trace and the attenuated reference pulse using complex trace analysis. An inverse problem for t^* is formulated to determine the relative t^* factor between the observation and the reference pulse. The use of instantaneous frequency to determine t^* has the advantage of incorporating the reference pulse spectrum into the estimation of t^*, similar to the use of spectral ratios [15].

An example of seismic refraction gather from the Ouachita PASSCAL experiment is shown in Figure 2. Although the amplitudes are unit normalized for plotting, both amplitudes and instantaneous frequencies can be extracted from the first arrivals. From the lowering in frequency of the first arrivals, the t^* values can be estimated.

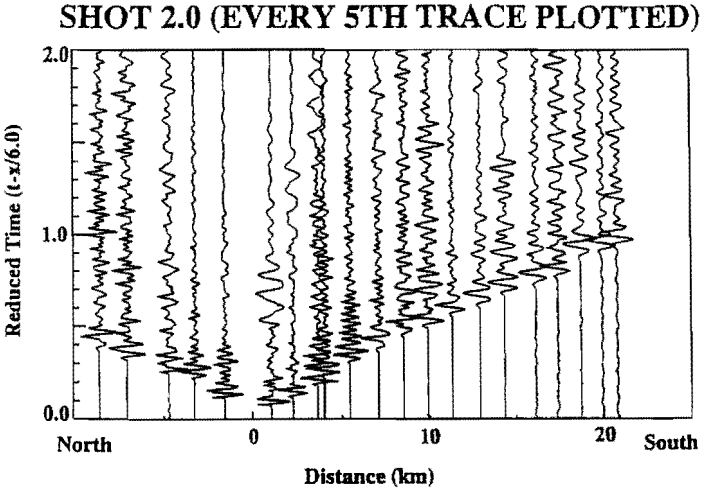

Fig. 2. *Observed crustal seismic gather displaying pulse broadening of the first arrivals.*

3. Ray Perturbation Analysis

Ray perturbation analysis can be utilized to perform sensitivity analysis for changes in the seismic attributes to variations in the model. For an initially homogeneous medium, ray perturbation results were obtained in [13], [17], [18], [20]. Farra and Madariaga [7] applied ray perturbation theory to compute travel-times and amplitudes in slightly perturbed media for a laterally varying initial medium. An application of ray perturbation theory to the inversion of travel-times and amplitudes was given in [22]. Interfaces were incorporated in [11], [22]. Jech and Psencik [12] used degenerate perturbation theory for the analysis of slightly anisotropic perturbations, and Nowack and Psencik [24] used this theory to obtain slightly anisotropic ray results for an initially isotropic, heterogeneous medium.

Snieder and Sambridge [29] investigated higher order travel-time perturbations using a Lagrangian approach and showed that second order travel-time perturbations could be obtained from first order ray perturbation analysis. The second order travel-time perturbation analysis was developed in [30], [31] for general ray coordinates, and [28] extended the analysis to higher order phase time perturbations.

In order to invert for seismic attributes, perturbation analysis of these attributes to medium variations is required. As a first step, the linearized ray equations can be written either in Cartesian coordinates or ray centered coordinates. In either case, the linearized ray equations can be used to determine the rays in the perturbed medium.

The first order travel-times can be obtained from Fermat's principle as an integration of the change in the slowness along the unperturbed ray paths, thus,

$$\delta T_1 = \int_0^{s_0} \delta u \, ds_0 + u_0 \dot{x}_i \delta x_i \Big|_0^{s_0} \quad , \tag{1}$$

where the last term on the right side is a boundary term related to the change in the ray endpoint positions [1]. The use of first order perturbations in travel-time tomography allows for significant savings as compared to more direct calculations of travel-time sensitivity. As a result, most recent tomographic inversion methods use first order analysis, and higher order terms are included into the inversion by iteration.

The second order travel-time perturbation has been obtained in [30] and can be written

$$\delta T_2 = \frac{1}{2} \int_0^{s_0} \delta x_i \left\{ R_i^{1S} + R_i^B \right\} ds_0 + B.T. \tag{2}$$

where B.T. represents the endpoint boundary terms, $R_i^{1S} = \dfrac{\partial \delta u}{\partial x_i} - \dfrac{d}{ds_o}\left[\delta u \dot{x}_i\right]$ is the slowness perturbation term, and $R_i^B = \dfrac{\partial u_0}{\partial x_i} - \dfrac{d}{ds_0}\left[u_0 \dot{x}_i\right]$ is the ray bending term used when the initial trajectory is not a true ray (see eq. (45) of [30]).

For the calculation of ray theoretical amplitudes, the dynamic, or paraxial ray equations can be used [4], [27]. The dynamic ray equations have also been applied to more general wavefield calculations, such as Gaussian beam summation and Maslov methods [2], [5], [6], [21]. To include ray amplitudes within an inversion, the sensitivity of geometric amplitudes to changes in the model must be obtained. Nowack and Lyslo [23] used ray perturbation methods to obtain the perturbed ray amplitudes, including geometric spreading and transmissions and reflections at interfaces and the free surface.

For realistic earth models, observed seismic amplitudes are also affected by attenuation of the medium. Anelastic calculations for slightly attenuative media can be obtained by an analytic continuation of the elastic wave solutions. For an effectively constant Q with frequency, an attenuated pulse can be written for positive frequencies as

$$p(x,\omega) = S(\omega)e^{i\omega(T-\ln(\omega/\omega_r)t^*/\pi)}e^{-\omega t^*/2} \tag{3}$$

where $T = \int u(x,\omega_r)ds$ is the travel-time along the ray, t^* is attenuation factor equal to $\int u(x,\omega_r)Q^{-1}(x)ds$, and $S(\omega)$ is the initial pulse spectrum. Using a first order linearized approach, attenuation is incorporated by computing t^* and the geometric spreading along a nearby real elastic ray instead of the true complex ray in the anelastic medium. For this case, the first order t^* perturbation to variations in the medium can be obtained in a similar fashion as the phase time perturbations [25].

4. Tomographic Inversion of Seismic Attributes

After seismic attributes have been extracted from the seismic wavefield data, an inversion of these attributes for velocity and attenuation structure can be performed. A linearized relation between variations in the slowness and inverse-q model parameters, δu and δq^{-1}, and the attribute residuals can be written

$$\begin{bmatrix} \delta T_R \\ \delta t^* \\ \delta \ln A \end{bmatrix} = \begin{bmatrix} \partial T_R/\partial u & \partial T_R/\partial q^{-1} \\ \partial t^*/\partial u & \partial t^*/\partial q^{-1} \\ \partial \ln A/\partial u & \partial \ln A/\partial q^{-1} \end{bmatrix} \begin{bmatrix} \delta u \\ \delta q^{-1} \end{bmatrix}, \tag{4}$$

where T_R is the complete real part of the travel-time, including dispersion from the attenuation model, t^* is the attenuation factor, and lnA is the ln-amplitude. Alternatively, the velocity could be used instead of the slowness.

For the causal, constant Q model described above, the imaginary part of the phase term is $i\omega T_R = i\omega\left(T - t^* \ln(\omega/\omega_r)/\pi\right)$, where T and t^* are both computed using the slowness at the reference frequency ω_r. This can be linearized in a fashion similar to [3]. The sensitivity of the real part of the travel-time T_R, including dispersion effects, is then

$$\frac{\partial T_R}{\partial u} = \frac{\partial T}{\partial u} - \frac{\partial t^*}{\partial u}\left(1+\ln(\omega_0/\omega_r)\right)/\pi, \quad \frac{\partial T_R}{\partial q^{-1}} = -\frac{\partial t^*}{\partial q^{-1}}\left(1+\ln(\omega_0/\omega_r)\right)/\pi, \tag{5}$$

where ω_r specifies the reference frequency at which the velocity model is referenced, and ω_0 is the frequency value for the linearization of the phase dispersion term. We use here the estimated instantaneous frequency of the observed pulse for ω_0. The partials of T and t^* are then obtained from the perturbation analysis of the preceding section.

The amplitude data are normalized to the amplitude of the reference pulse for a near offset receiver. The amplitude partials can be written as

$$\frac{\partial \ln A}{\partial u} = \frac{\partial \ln A_g}{\partial u} + \frac{\partial \ln A}{\partial t^*}\frac{\partial t^*}{\partial u}, \qquad \frac{\partial \ln A}{\partial q^{-1}} = \frac{\partial \ln A}{\partial t^*}\frac{\partial t^*}{\partial q^{-1}}, \tag{6}$$

where $\ln A_g$ is the natural log of the geometric spreading component of the amplitude related to the real velocity or slowness model.

Iterative inversion techniques [26] can then be used to solve eq. (4). This is a damped iterative inversion rather than a more formal stochastic inversion since, in the procedure followed here, the model parameterization can change at each iteration. This allows for a small number of model parameters in the starting iterations representing a smooth model, and an increasing number of model parameters at higher iterations. The iterative procedure is terminated when the data residuals are within the estimated data uncertainties. At this stage, no further improvement in the model is warranted given the data. An approximate estimate of the uncertainties in the model parameters can then be obtained at the final iteration.

In the procedure described above, a sequence of linearized inversions is performed from smooth to less-smooth models. This is done by increasing the number of model parameters at each iteration step. The iterative procedure is then terminated when the data residuals are within the observed data uncertainties. This type of iterative procedure has the advantage of progressively constraining the longer wavelength features of the model based on fitting of the data. If smooth model interpolations are used, such as by using splines, this procedure provides damping as well as smoothing of the solution.

5. Applications to Crustal Refraction Data

As a first example of the inversion of seismic attributes, an inversion for shallow crustal structure has been performed along the northern end of the PASSCAL Ouachita seismic experiment recorded in Arkansas [14], [25]. An iterative sequence of inversions has been performed from smooth to less-smooth models by increasing the number of vertical speed lines in the model at each iteration step. As a first step, a vertically varying starting model derived from a 1-D inversion was used to start the iterative process. The model had five vertical nodes at depths of 0, .75, 1.5, 2.25 and 3.25 km. The iteration sequence initiated with two horizontal speed lines and then progressed to three, five, and finally nine equally-spaced vertical speed lines with distances between 0 to 80 km. The resulting final model with nine vertical speed lines had 45 velocity nodes and 45 attenuation nodes. For this example, velocity, instead of slowness, was used to represent the elastic structure. The iterative process was terminated when the average data residuals for all the seismic attributes were smaller than the observed data uncertainties. This type of procedure estimates the longer wavelength features of the model based on fitting of the data. The iterative process was found to be important when performing simultaneous inversions of different seismic attributes. In particular, amplitudes were found to be very sensitive to model roughness, and smooth models were required.

The final inverted velocity or inverse-slowness model with nine vertical speed lines is shown in Figure 3A and includes a shallow basin deepening with distance to the south. This is also imaged in the attenuation, or inverse-q model, shown in Figure 3B. The attenuation model has q values as low as 20 near the surface, increasing to values

In the second example, a simultaneous inversion for velocity and attenuation using seismic attributes was applied to refraction data from the Glimpce Lake Superior experiment. One component of the Glimpce experiment involved recording a 250 km long wide-angle refraction profile, which extends across Lake Superior from North to South (Figure 5). Data from four ocean bottom and two land based seismometers were used from the experiment to calculate seismic attributes.

The seismic attributes, including amplitudes, differential t^* values and phase times for first arrivals, were then used to invert for velocity and attenuation. An iterative procedure from smooth to less-smooth models was performed similar to that in the previous example. This was found to be important when including different seismic attributes in the inversion. The inversion was terminated when the RMS residuals for all

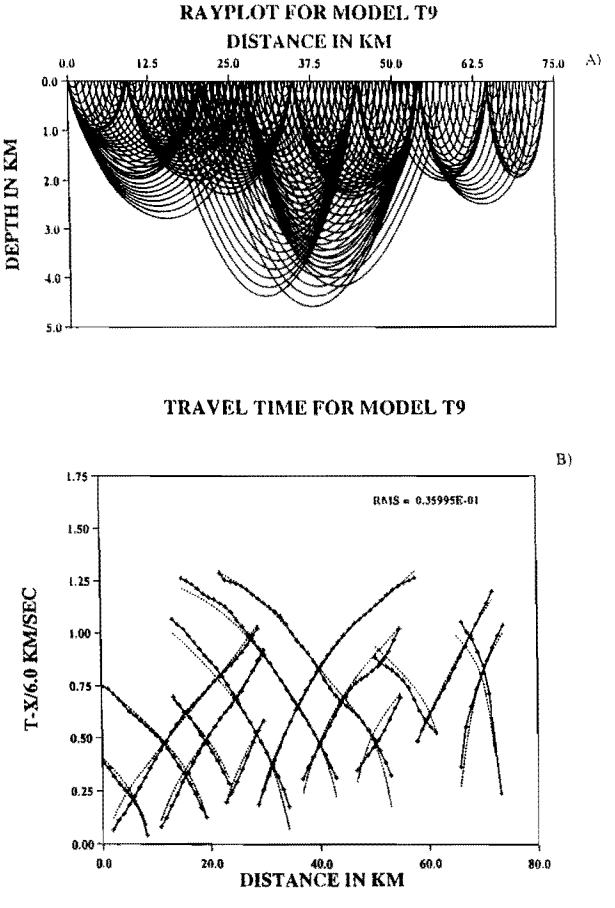

Fig. 4. *A) The ray diagram for the crustal model shown in Figure 3. B) Observed and computed travel-times for the crustal model shown in Figure 3.*

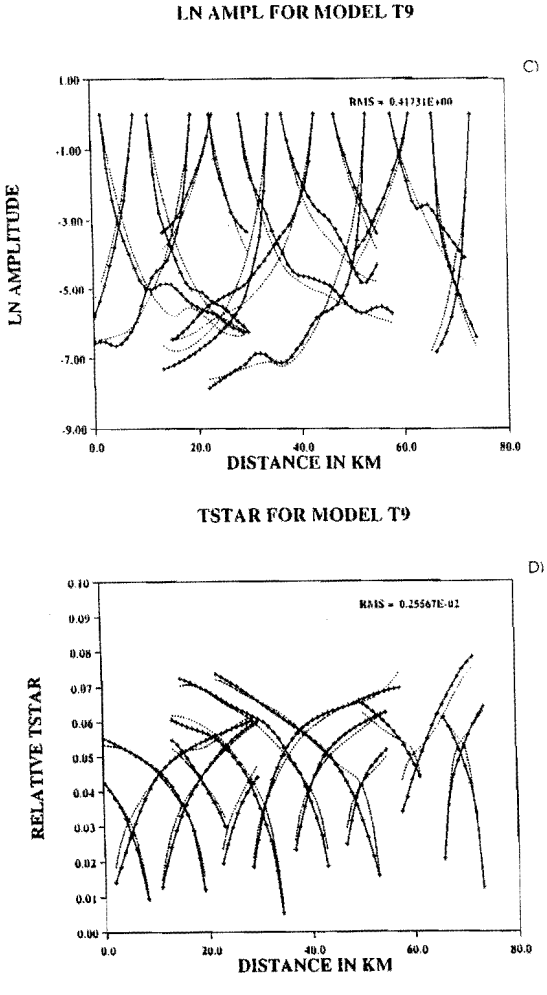

Fig. 4 (cont.). *C) Observed and predicted ln-amplitudes. D) Observed and predicted t^* values. The RMS residuals are shown in the upper right for each data attribute. For each attribute, the observed data is shown with crosses and the predicted data by dashed lines.*

attributes were within the data uncertainties. The final model for velocity and attenuation is shown in Figure 6. The inverted velocity model is displayed in Figure 6A and shows a central rift basin along with a northern basin. This structure is also imaged in the inverse-q attenuation structure shown in Figure 6B. Figure 7 shows the observed and predicted travel-times, ln-amplitudes, and differential t^* values for the final 119 node model. For a geological discussion of the inversion results in Figure 6 see [16].

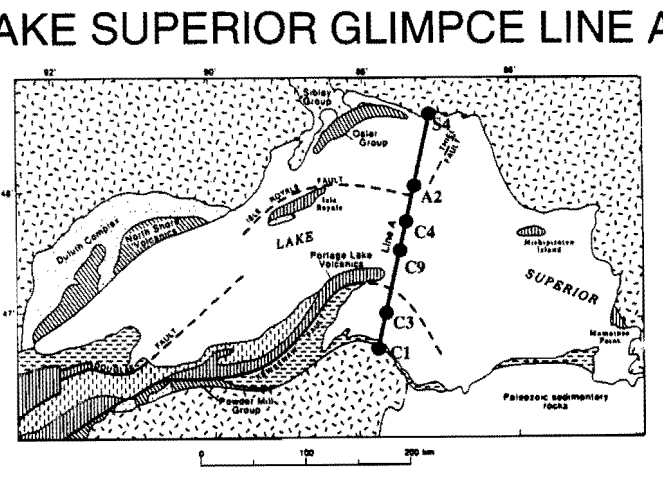

Fig. 5. *Map of the Lake Superior area showing the location of line A of the GLIMPCE experiment. Seismometer locations S4 and C1 are land based seismometers and A2, C4, C9 and C3 are lake bottom seismometers.*

In each of the above examples, the seismic amplitudes were found to be very sensitive to the model roughness. The sensitivity of ray amplitudes was noted previously by [22], who suggested that geometric amplitudes could be used to resolve smaller scale features than could be determined from travel-times alone. This was also concluded in [19]. However, from the observed crustal data used for the examples here, the inverted models were required by the observed amplitudes to maintain a relatively smooth character. A large parameter travel-time inversion alone would have fit the travel-time data, but would have predicted ray amplitudes too rough as compared to the observed amplitudes. Thus, the inversion of the amplitudes for these data sets required that an iterative procedure from smooth to less-smooth models be performed. Also, amplitudes and t^* values were required to be included, along with travel-times, at each step of the inversion in order to fit all the seismic attributes at the final iteration.

6. Conclusions

An inversion formulation using seismic attributes has been developed which includes more of the seismic data than just travel-times, but with less sensitivity to noise than a complete wavefield inversion. The seismic attributes considered include envelope amplitudes, instantaneous frequencies, and phase times of selected arrivals. Instantaneous frequencies are converted to attenuation factors t^* using a matching procedure between the data and near offset reference pulses. This compensates for the effects of reference pulse spectrum in the estimation of the attenuation factors.

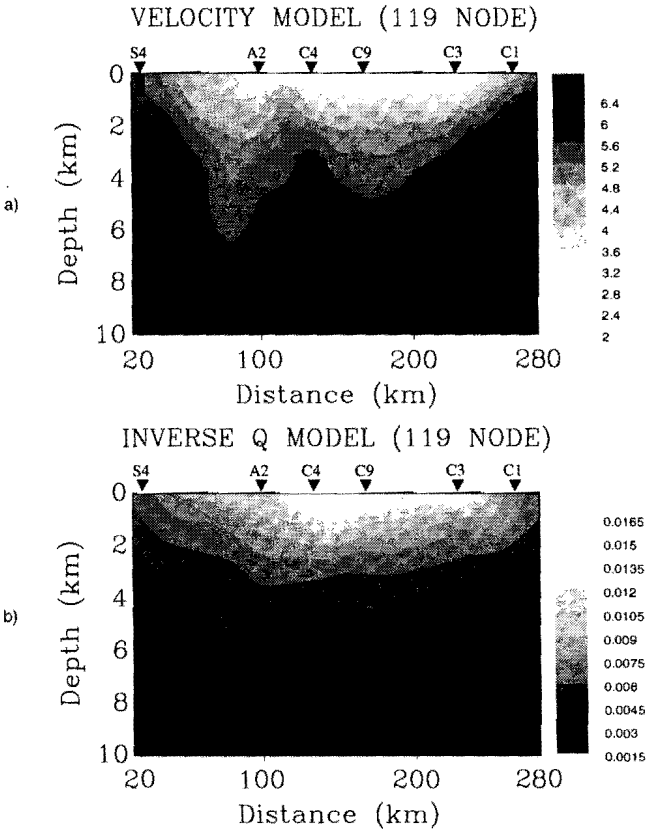

Fig. 6. *A) Velocity model for the 119 node final model for GLIMPCE lineA. B) Attenuation model for the 119 node final model.*

An iterative inversion procedure was performed, starting with smooth models and progressing to less-smooth models. This type of inversion procedure was found to be important when simultaneously inverting different seismic attributes. Only first order perturbations of the different seismic attributes were used at each iteration so that the order of perturbation for the different seismic attributes at each iteration would be kept the same. Higher order perturbations of the seismic attributes were incorporated using multiple iterations.

To illustrate the inversion of seismic attributes in laterally varying media, observed crustal refraction data from the Ouachita PASSCAL and Glimpce Lake Superior experiments have been used to invert for crustal structure. The amplitude data were found to be very sensitive to the roughness of the model. However, for the example refraction data used, the models were required by the amplitudes to maintain a relatively smooth character. The amplitudes predicted by a travel-time inversion alone, using a

large parameter model without smoothing, would have been too rough. Thus, the amplitude and t^* data needed to be included along with the travel-times at each step of the inversion in order to fit all the seismic attributes at the final iteration.

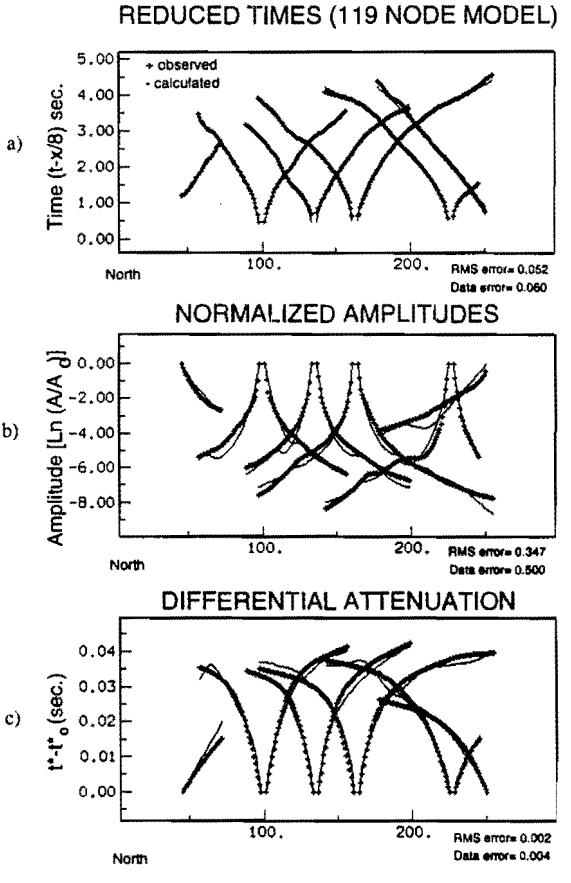

Fig. 7. *A) Observed and calculated travel-times for the 119 node final model. B) Observed and calculated amplitudes for the final model. C) Observed and calculated differential attenuation values for the final model.*

References

[1] K. Aki and P. G. Richards, *Quantitative Seismology Theory and Methods* , W.H. Freeman, San Francisco, CA, 1980.

[2] V. Cerveny, *Gaussian beam synthetic seismograms*, J. Geophys., 58 (1985) 44-72.

[3] V. Cerveny and A. Frangie, *Effects of causal absorption on seismic body waves*, Studia geoph. et geod., 26 (1982) 239-253.

[4] V. Cerveny and F. Hron, *The ray series method and dynamic ray tracing system for 3-D inhomogeneous media*, Bull. Seism. Soc. Am. 70 (1980) 47-77.

[5] V. Cerveny, M. M. Popov, and I. Psencik, *Computations of wavefields in inhomogeneous media - Gaussian beam approach*, Geophys. J.R. astr. Soc., 70 (1982) 109-128.

[6] C. H. Chapman and R. Drummond, *Body-wave seismograms in inhomogeneous media using Maslov asymptotic theory*, Bull. Seism. Soc. Am., 72 (1982) S277-S317.

[7] L. Cohen, *Time-Frequency Analysis*, Prentice-Hall, Englewood, Cliffs, NJ1995.

[8] I. Daubechies, *Ten Lectures on Wavelets*, SIAM, Philadelphia, PA, 1992.

[9] V. Farra and R. Madariaga, *Seismic waveform modeling in heterogeneous media by ray perturbation theory*, Geophys. J.R. astr. Soc., 76 (1987) 697-712.

[10] V. Farra, R. Madariaga, and J. Virieux, *Comment on "The ambiguity in ray perturbation theory" by Roel Snieder and Malcolm Sambridge*, J. Geophys. Res., 99 (1994) 21963-21968.

[11] V. Farra, J. Virieux, and R. Madariaga, *Ray perturbation theory for interfaces*, Geophys. J. Int., 99 (1989) 2697-2712.

[12] J. Jech and I. Psencik, *First order perturbation method for anisotropic media*, Geophys. J. Int., 99 (1989) 369-276.

[13] J. B. Keller, Wave propagation in random media, *Proc. Symp. Appl. Math.*, 13 (1962) 227-246.

[14] W. J. Lutter, R. L. Nowack, and L. W. Braile, *Seismic imaging of upper crustal structure using travel times from the PASSCAL Ouachita experiment*, J. Geophys. Res., 95 (1990) 4621-4631.

[15] M. P Matheney and R. L. Nowack, *Seismic attenuation values obtained from instantaneous frequency matching and spectral ratios*, Geophys. J. Int., 123 (1995) 1-15.

[16] M. P. Matheney, R. L. Nowack, and A. M. Trehu, A.M., *Seismic attribute inversion for velocity and attenuation structure using data from the Glimpce Lake Superior experiment*, J. Geophys. Res., (1996) submitted.

[17] B. J. Moore, *Seismic ray theory for lithospheric structures with slight lateral variations*, Geophys. J.R. astr. Soc., 63 (1980) 671-689.

[18] _____, *Seismic rays in media with slight lateral variations in velocity*, Geophys. J. Int., 105 (1991) 213-227.

[19] F. Neele, J. Van Decar, and R. Snieder, *The use of P wave amplitude data in a joint inversion with travel times for upper mantle velocity structure*, J. Geophys. Res., 98 (1993) 12033-12054.

[20] S. J. Norton and M. Linzer, *Correcting for ray refraction in velocity and attenuation tomography: a perturbation approach*, Ultrason. Imag., 4 (1982) 201-233.

[21] R. L. Nowack and K. Aki, *The 2-D Gaussian beam synthetic method: testing and application*, J. Geophys. Res., 89 (1984) 7797-7819.

[22] R. L. Nowack and W. J. Lutter, *Linearized rays, amplitude and inversion*, Pure and Applied Geophys., 128 (1988) 401-421.

[23] R. L. Nowack and J. A. Lyslo, *Frechet derivatives for curved interfaces in the ray approximation*, Geophys. J. Int., 97 (1989) 497-509.

[24] R. L. Nowack and I. Psencik, *Perturbation from isotropic to anisotropic heterogeneous media in the ray approximation*, Geophys. J. Int., 106 (1991) 1-10.

[25] R. L. Nowack and M. P. Matheney, *Inversion of seismic attributes for seismic velocity and attenuation*, Geophys. J. Int., (1996) submitted.

[26] C. C. Paige and M. A. Saunders, *LSQR: an algorithm for sparse linear equations and sparse least squares*, Assn. Comp. Mach. Trans. Mathematical Software, 8 (1982) 43-71.

[27] M. M. Popov and I. Psencik, *Computation of ray amplitudes in inhomogeneous media with curved interfaces*, Studia Geophys. Geol., 22 (1978) 248-258.

[28] R. Snieder and D. F. Aldridge, *Perturbation theory for travel times*, J. Acoust. Soc. Am., 98 (1995) 1565-1569.

[29] R. Snieder and M. Sambridge, *Ray perturbation theory for traveltimes and ray paths in 3-D heterogeneous media*, Geophys. J. Int., 109 (1992) 294-322.

[30] R. Snieder and M. Sambridge, *The ambiguity of ray perturbation theory*, J. Geophys. Res., 98 (1993) 22021-22034.

[31] R. Snieder and C Spencer, *A unified approach to ray bending, ray perturbation and paraxial ray theories*, Geophys. J. Int., 115 (1993) 456-470.

[32] M. T. Taner, F. Koehler, and R. E. Sheriff, *Complex seismic trace analysis*, Geophysics, 44 (1979) 1041-1063.